JOURNAL OF PROPULSION AND POWER
Vol. 17, No. 6, November–December 2001

Experimental Study of Scramjet Module

Marat A. Goldfeld* and Alexey V. Starov†
Russian Academy of Sciences, 630090, Novosibirsk, Russia
and
Viacheslav V. Vinogradov‡
Central Institute of Aviation Motors, 111250, Moscow, Russia

Results of an experimental study of three-dimensional inlets and a scramjet module are presented. The scramjet module consists of an inlet and a combustion chamber. The module is designed to study the flow structure, to obtain the inlet performance, and to study the mutual effects of the combustor and the inlet, fuel ignition and combustion (hydrogen and hydrocarbon fuels), and the efficiency of various methods of fuel injection. The tests were conducted in a blowdown wind tunnel at Mach numbers from 2 to 6 and unit Reynolds numbers from 8 to 54 $\times 10^6$ and in the hot-shot wind tunnel at Mach numbers M_∞ = 6 and 7.2 and unit Reynolds numbers from 1.4 to 45 $\times 10^6$.

Nomenclature

A_0	=	inlet entrance area, $H \times B$
A_∞	=	captured jet area
B	=	inlet entrance width
f	=	flow rate coefficient, A_∞ / A_0
H	=	inlet entrance height
M	=	Mach number
P	=	pressure
Re	=	Reynolds number
T	=	temperature
δ, δ^*, δ^{**}	=	boundary layer, displacement, and momentum thickness, respectively
ν	=	pressure recovery coefficient

Subscripts

p	=	pitot pressure
t	=	total parameters
th	=	throat
w	=	wall
∞	=	freestream parameters

Introduction

THE development of hypersonic flying vehicles with airbreathing propulsion is an important problem because their use for various practical purposes seems very promising. An integral part of this problem is the development of hypersonic air-breathing engines (scramjets) for this vehicle. The inlet is one of the basic parts of such an engine. Thus, scramjet studies focus much interest in the study of hypersonic inlets of various types and applications.

The scramjet inlet must ensure engine operation up to high hypersonic flight speeds, which correspond to Mach numbers M_∞ =10–12 and higher. At these high speeds, traditional two-dimensional and axisymmetric inlets have severe drawbacks. One of the most complicated problem is the heat protection of compression surfaces, especially in the region of duct entrance and near the throat.[1] Another complicated problem is the necessity of decreasing the wave drag of the inlet with external compression at transonic speeds.

Much attention has been paid lately to three-dimensional inlets that are built using a combination of two-dimensional flows in such a way that the cross sections of the captured stream are compressed along converging intersecting directions. Inlets of this type are called convergent inlets (CI).[2] They allow one to obtain compact cross sections of the duct entrance and the throat. The CIs were constructed by gasdynamic design methods using portions of internal supersonic flows converging toward the symmetry axis. In Ref. 3 the CIs were built by spatial combinion of two-dimensional flows with oblique shock waves of general spatial location.

Another configuration of three-dimensional inlets, which may be considered a CI, is presented in Ref. 4. The surfaces forming the duct walls and the cowl had swept edges (45 deg), and the inclination angles of the compression surfaces were not very large (3–6 deg). The inlet duct was separated into several regions by three struts that also had swept leading and trailing edges. The compression process was completed in the channels between the struts. The struts could be used for fuel injection. Note that this construction had a less compact entrance than an axisymmetric CI, but it is more flexible in the formation and control of the throat area. Three-dimensional inlets of this and another types were also studied at the Central Institute of Aviation Motors (CIAM).[5]

Theoretical and experimental studies of two models of three-dimensional inlets were studied jointly by the Institute of Theoretical and Applied Mechanics, Siberian Branch, Russian Academy of Science (ITAM SB RAS) and CIAM.[6] The models were tested in two positions: in the flow core and on the wind-tunnel wall. The second variant of model position allowed for simulating a thick boundary layer on the front part of the fuselage by using the boundary layer on the wind tunnel wall.

Model 1 (Fig. 1), in contrast to Ref. 4, had one adjustable strut, which allowed relative throat area to vary between 0.126 and 0.316. The side walls and the strut had a back sweep of 45 deg. It was found that such an inlet had a comparatively low flow rate coefficient $f(M)$ and a small starting range.[6]

Model 2 was a modification of the first one. It did not have a strut, and the inlet was adjusted by discrete longitudinal motion of the cowl. Symmetric side walls of the model had a forward sweep of 45 deg, and the relative throat area was 0.358. The testing of this model allowed one to obtain satisfactory characteristics of the inlet in experiments in the flow core ($\delta = 0$), but a dramatic reduction of the flow rate and total pressure recovery coefficients was observed if there was a thick boundary layer at the inlet duct entrance.[6]

Based on the test results for these models, an engine module was developed (model 3). It was supposed to use the favorable influence of blended sweep on inlet starting and flow rate characteristics.

Received 4 June 2000; accepted for publication 29 December 2000.

*Senior Research Scientist, Institute of Theoretical and Applied Mechanics (ITAM), Siberian Branch, 4/1 Institutskaya Street; Gold@Itam.nsc.ru.

†Research Scientist, Institute of Theoretical and Applied Mechanics (ITAM), Siberian Branch.

‡Department Head, 2 Aviamotornaya Street; slava@postman.ru. Member AIAA.

The following objectives were pursued in testing the engine module.

1) Obtain flow rate characteristics based on flow parameters at the combustion chamber exit.

2) Determine the total pressure recovery coefficient and flow Mach number in the inlet throat.

3) Determine the inlet starting conditions and flow formed in the duct using schlieren pictures and oil-film visualization.

4) Determine the influence of a thick incoming boundary layer on inlet starting, flow structure in the duct, and integral characteristics.

5) Determine the pressure fields in the inlet and combustor.

Model and Experimental Technique

The inlet of model 3 had swept forward side walls and a central strut with sweep back (Fig. 2). To approach the full-scale size and to take into account the model symmetry about the strut, the inlet was made as a half-model.

A scheme and basic dimensions of the developed scramjet model are shown in Fig. 3. The bluntness radius of all leading edges was 1 mm.

The model construction allows for fuel injection into the combustor during combustion tests in a hot-shot wind tunnel. The fuel is proposed to inject through a group of injectors (Fig. 2) mounted on an insert that is placed in a rectangular window on the strut (experimental studies were performed without injectors on a smooth wall). To make injection more uniform and to avoid duct blockage, the injectors are located in two bearings with respect to the horizontal plane passing approximately through the middle of the inlet height. Each injector has four orifices for fuel injection. They are located on a swept strut along the model duct width. It is also possible to install windows in the strut and side wall for visualization of the flow and fuel combustion.

The model had 149 static pressure taps for static pressure measurements on internal stagnation surfaces and on the cowl. The largest number of static pressure taps was positioned in the inlet throat and combustion chamber, which are most important from the viewpoint of inlet starting control and stable combustion.

The pitot pressure in the inlet throat, for determining the total pressure recovery coefficient, was measured by a rake that had eight pressure probes positioned uniformly over the throat height. To determine the airflow rate at the model exit, there was a rake with 32 pressure probes located uniformly over the height and width of the exit cross section of the model. Four static pressure probes were located on internal surfaces of the model in close vicinity of the rake.

The main series of tests was performed in blowdown wind tunnel T-313 of ITAM SB RAS with test section size 600 × 600 × 2000 mm at Mach numbers from 2 to 6. The test conditions are presented in Table 1.

The tests were performed for two variants of model mounting in the test section. In the first case, it was mounted on a strut in the flow

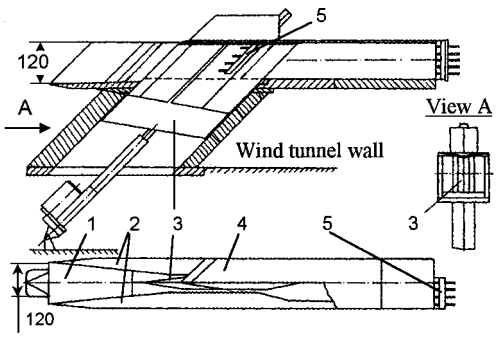

Fig. 1 Adjustable inlet with sweep flat walls: 1) model base, 2) side walls, 3) adjustable strut, 4) cowl, and 5) pitot pressure rakes.

Table 1 Test parameters in wind tunnel T-313

M_∞	$P_{t\infty}$, MPa	T_t, K	$Re_l \times 10^6$, 1/m	$\delta = 0$	$\delta > 0$
2	0.200	290	25.59	+	−
2.5	0.260	275	28.55	−	+
3	0.430	284	35.22	+	+
4	1.058	284	52.49	+	+
6	0.810	425	8.95	+	+

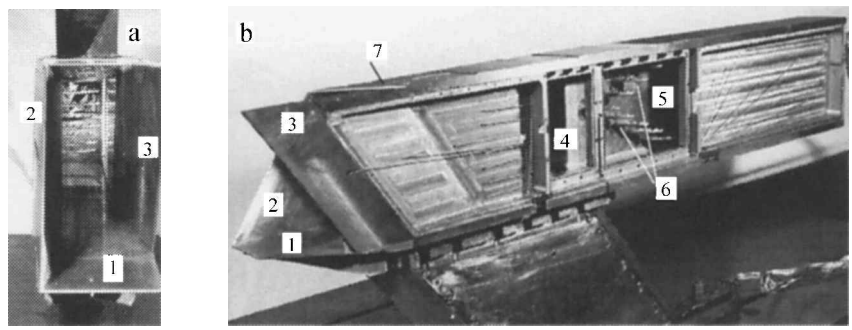

Fig. 2 Photographs of scramjet model: 1) model base, 2) right wall (strut), 3) left wall, 4) window, 5) combustion chamber, 6) fuel injector ramps, and 7) cowl: a) front view and b) side view.

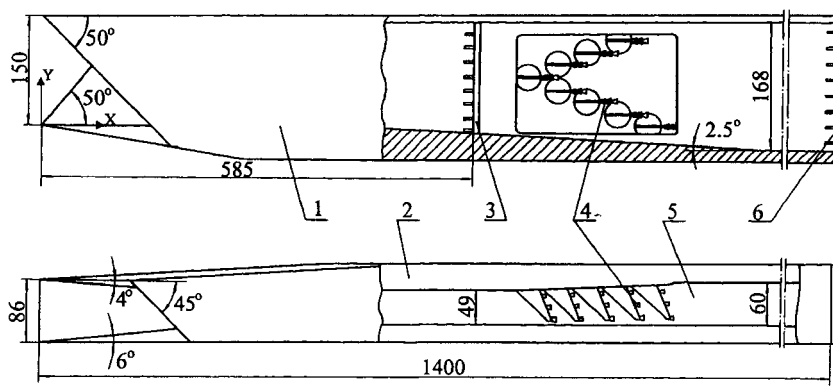

Fig. 3 Scheme of scramjet module: 1) left wall, 2) right wall (strut), 3) six total pressure rakes, 4) fuel injectors, and 5) model base.

Table 2 Characteristics of the boundary layer on the wind tunnel wall (T-313)

M	δ, mm	δ^*, mm	δ^{**}, mm	δ/H	δ^*/H
3	18.15	4.2	0.95	0.121	0.028
4	39.2	11.36	1.65	0.261	0.076
6	43.04	15.7	3.1	0.287	0.105

Table 3 Test parameters in wind tunnel IT-302

M_∞	$P_{t\infty}$, MPa	T_t, K	$Re_l \times 10^6$, 1/m	$\delta = 0$	$\delta > 0$
6	12.43–1.60	2566–1475	7.04–1.41	+	–
7.2	44.52–7.75	2382–1259	19.76–5.20	+	–

core of the wind tunnel and there was no boundary layer at the inlet entrance ($\delta = 0$). In the second case, the model was mounted on the wind-tunnel wall with a special transitional plate, which allowed for diverting a thick boundary layer of the wind tunnel to the inlet entrance to simulate the boundary layer on the vehicle forebody upstream of the engine duct entrance ($\delta > 0$). The boundary layer-thickness on the wind tunnel wall amounted to 29% of the model duct height at high Mach numbers. The characteristics of the boundary layer (thickness, displacement thickness, momentum thickness) on the wind tunnel wall are presented in Table 2.

Schlieren visualization of the flow over the model entrance and the oil-film visualization of the limiting streamlines at the entrance were also performed.

The experiments at $M = 6$ and 7.2 were conducted in the hot-shot wind tunnel IT-302M of ITAM SB RAS with nozzle exit diameter of 300 mm and test section length of 1000 mm. The test conditions are presented in Table 3.

The measurement errors were 1–2% for measurements in the blowdown wind tunnel T-313 and 3–4% for measurements in the hot-shot wind tunnel IT-302M.

Results and Discussion

An analysis of the pressure distribution shows that it is highly non uniform. An example of the static pressure distribution over the inlet throat perimeter at $M = 6$ is shown in Fig. 4. It is seen that especially strong nonuniformity is observed on the strut. This can be related to the boundary-layer separation caused by the action of a more intense shock wave because the inclination angle of the side wall surface is larger than the corresponding angle of the strut inclination by a factor of 1.5. This conclusion is also supported by considerable pressure nonuniformity in the presence of a thick boundary layer at the inlet duct entrance. Similar results were obtained for all Mach numbers when the inlet was started. For subsonic flow regimes in the throat, the pressure field was more uniform.

When analyzing the pressure distribution along the model (Fig. 5 and 6), we can see an alternation of pressure peaks typical of supersonic duct flow, which is due to the alternation of shock waves and expansion waves. This nonuniformity is also observed when decreasing the Mach number, but retaining a supersonic flow in the model duct. Figure 7 shows the features of a flow at the inlet channel entrance when the inlet was started.

If the inlet was not started, the pressure equalizes both along the duct and over the inlet throat perimeter. For $M_\infty < 2.5$, the inlet was started neither in the flow core nor on the tunnel wall. This was confirmed by the schlieren pictures (Fig. 8) which show the normal shock wave and intensive spillage before the inlet entrance. The oil-film visualization of the streamlines also confirms that the inlet was not started (Fig. 9). It is seen that the flow at the inlet entrance has a complex structure with the large nonsymmetrical vortelces close to a side wall and a strut. The nonstarting of inlet causes the large separation of boundary layer on the wind tunnel wall before the inlet forward edge. For $M_\infty > 3$, the thick boundary layer had a strong effect on the character of static pressure distribution and pressure level in the duct.

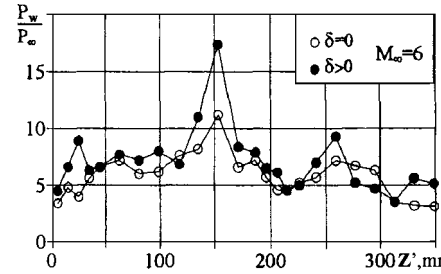

Fig. 4 Static pressure over the inlet throat perimeter (base, strut, cowl, side wall).

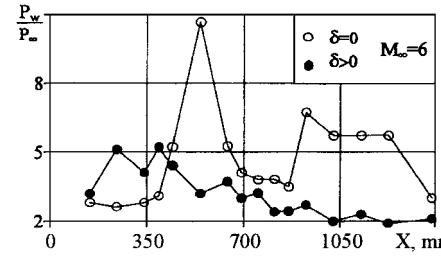

Fig. 5 Static pressure distribution along the strut.

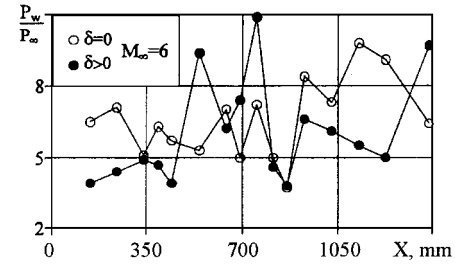

Fig. 6 Static pressure distribution along the side wall.

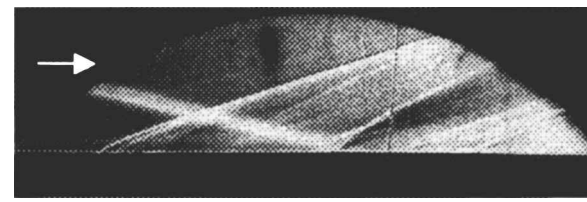

Fig. 7 Schlieren picture of starting inlet.

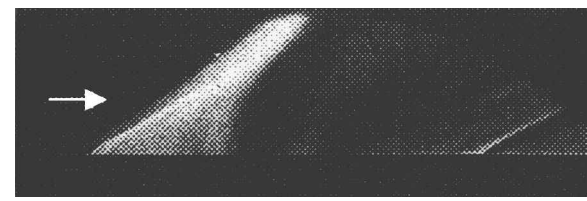

Fig. 8 Schlieren picture of nonstarting inlet.

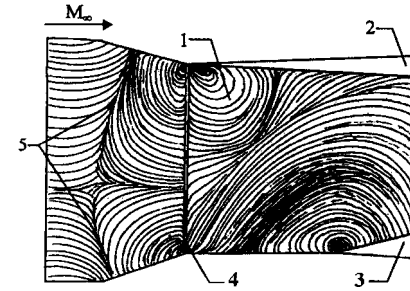

Fig. 9 Oil-film visualization of nonstarting inlet: 1) model base, 2) strut, 3) left wall, 4) leading edge, and 5) boundary-layer separation on wind-tunnel wall before the inlet.

Because of model asymmetry, this effect was different at the opposite compression surfaces. Thus, the pressure equalization and reduction of the overall pressure level along the duct were observed at $M_\infty = 6$ on the strut (Fig. 5). A typical saw-tooth distribution of static pressure was observed on the side wall (Fig. 6), though there was some shift along the model and some increase of peak pressure values. This is probably due to the appearance and growth of local separation regions.

An example of pitot pressure distribution in the inlet throat for $M_\infty = 4$ and 6 is shown in Fig. 10. A strong pressure nonuniformity over the duct height can be noted, as well as a steplike character of pressure distribution in a supersonic duct flow, especially in the lower part of the throat approximately up to half of its height. The pressure distribution was qualitatively changed at the flow breakdown. This is manifested in the smoothing of the pressure peaks at $M_\infty = 3$, and the character of pressure distribution approaches typical of a near-wall turbulent layer (for $M_\infty < 3$). This result is apparently determined to a large extent by the boundary-layer separation at the model base. The presence of separation is also supported by the static pressure distribution at the base along the model duct. Figure 8 also shows the influence of a thick boundary layer upstream of the model on the pitot pressure variation in the inlet model throat (black markers), which leads to pressure reduction, mainly at the model base. Also a decrease in pressure profile nonuniformity is observed (for $\delta > 0$), which is most appreciable when the freestream Mach number was decreasing. A field of pitot pressure at the model exit had a complicated structure, which depended on Mach number and position of the model in the flow core or on the wind-tunnel wall. An example of pressure field is shown in Fig. 11 for Mach 6.

As already noted, this model is an engine module that has an inlet and combustion chamber with a system for fuel injection. This allows one to perform combustion tests in a hot-shot facility. Because there is always the problem of identification of measurement results in different wind tunnels, moreover, in principally different wind tunnels such as T-313 (blowdown wind tunnel) and IT-302M (hot-shot facility), the experiments were performed for Mach number 6 and similar Reynolds numbers. The results of static pressure measurements on external compression surface at nonseparated flow obtained in wind tunnels with blowdown and short operation regimes are in fairly good agreement with each other.[1] An example of pitot pressure distribution in the model throat for Mach 6 and 7.2 in the hot-shot wind tunnel IT-302M is presented in Fig. 12.

For comparison, Fig. 12 shows the pitot pressure profile in the throat for $M_\infty = 6$ obtained in the main series of tests in the blowdown wind tunnel T-313. A difference in pressure profiles obtained in these two wind tunnels is apparently caused by boundary-layer separation on the side walls of the model by influence of shock waves. The appearance of separation is caused by substantially different temperature regimes of the model surface and, hence, by different states of a boundary layer.[7] For tests in the blowdown wind tunnel, an "adiabatic" wall was observed, but for the hot-shot wind tunnel the wall temperature factor T_w/T_t, was 0.15–0.2. Hence, the intensity of separation and deceleration of the flow in the first case was larger and caused corresponding changes of pitot pressure profiles.

An adjustment of throat area (model 1) allows obtaining high static pressure ratios (Fig. 13). The effect of the adjustment increases with the increase of Mash number, especially at Mach numbers higher than 3. These data show that it is necessary to undertake efforts to increase static pressure ratio. The results of static and pitot pressure measurements made it possible to estimate the mean Mach number in the inlet throat as a function of the freestream velocity (Fig. 14). These calculations were based on averaging the pitot and static pressures over the model cross section. Because the fields of pitot and static pressures are strongly nonuniform, one has to bear in mind a possible error when determining the Mach number in the duct. This error can be caused by boundary-layer separation

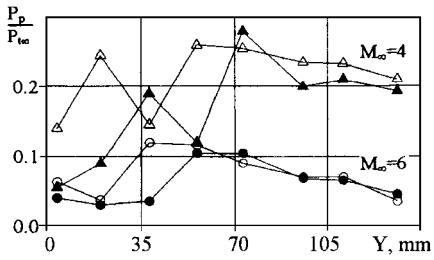

Fig. 10 Pilot pressure in the inlet throat.

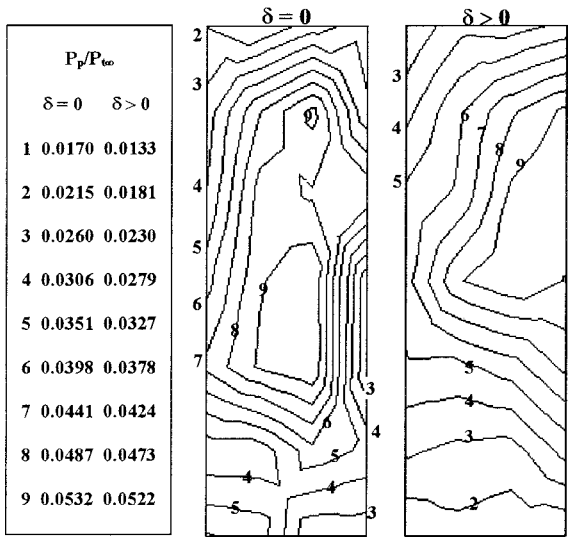

Fig. 11 Pilot pressure isolines at model exit, $M_\infty = 6$.

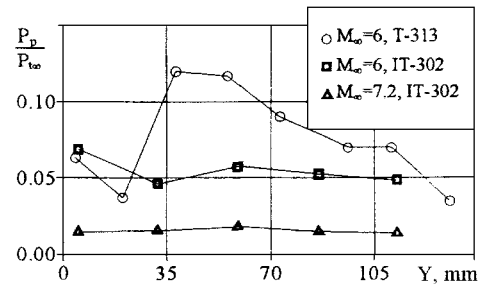

Fig. 12 Inlet throat pitot pressure distribution in different wind tunnels.

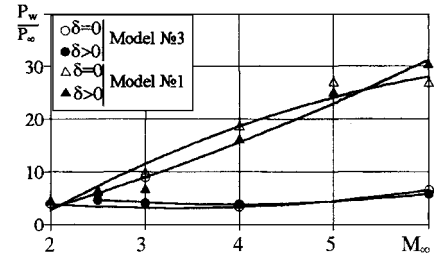

Fig. 13 Static pressure ratio in the model throat.

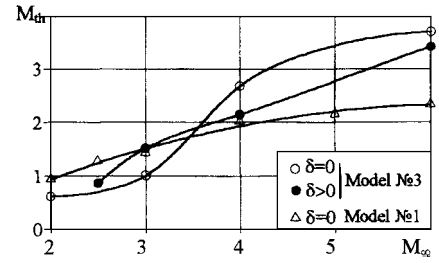

Fig. 14 Throat Mach numbers.

on the walls of the inlet. This could be the reason for obtaining an underestimated Mach number in the throat for $M_\infty = 3$ ($\delta = 0$). This follows from the analysis of the pressure distributions and schlieren pictures. These data show that the inlet is started at $M_\infty = 3$ in the flow core and nonstarting in the presence of a thick incoming boundary layer.

Figure 14 shows the Mach numbers in the throat of a three-dimensional inlet with adjustable central strut.[6] It can be concluded on the basis of these data that for smaller stagnation parameters of the flow a blended swept configuration allows one to have supersonic airflow at the entrance of the combustion chamber beginning from comparatively low freestream Mach numbers, that is, the flow velocity at the duct exit of such an inlet allows one to supply the maximum possible energy with minimum total pressure losses.

Based on measurements performed in the throat, the pressure recovery coefficient was determined (Fig. 15). It is seen that the pressure recovery coefficient in a blended swept inlet remains rather high up to $M_\infty = 6$, even in the presence of a thick incoming boundary layer. The level of the pressure recovery coefficient of model 3 is close to the level of the pressure recovery coefficient of an adjustable inlet in the flow core at Mach number greater than 4.

When the pitot pressure fields at the exit were measured, it was established that the pressure was strongly nonuniform both in the vertical and horizontal directions. It was retained for all Mach numbers and both variants of model mounting in the wind tunnel. It is known that this nonuniformity in pressure distribution can lead to considerable errors in determining the airflow rate through the inlet. When the number of pitot pressure probes was increased up to 7–10 and more, however, it is possible to reach an accuracy of flow rate determination better than 3%. The averaging of pitot and static pressures over the areas was used. Based on these data, the flow rate coefficient vs the Mach number was determined (Fig. 16).

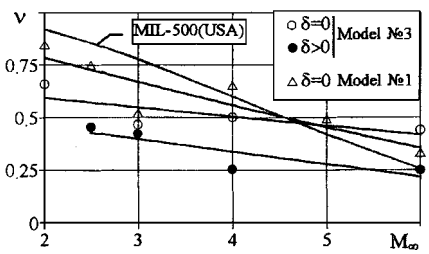

Fig. 15 Pressure recovery coefficient.

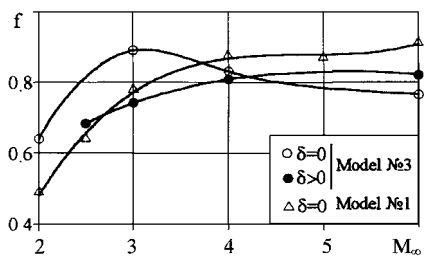

Fig. 16 Flow rate coefficient.

Beginning at $M_\infty = 4$, the flow rate coefficient of the inlet of given configuration is slightly lower than that of previously tested inlets, however, its value is quite acceptable and practically independent of the presence of boundary layer, similar to a swept forward inlet. The dependence of flow rate vs M_∞ is unusual, but explainable with increase in M_∞, the pressure gradients are increased, but the state of the boundary layer becomes closer to transient and laminar. The latter caused more intensive separation of the boundary layer and larger spillage of flow before the cowl. For tests with incoming boundary layer, the negative effect of boundary layer laminarization at large M_∞ was compensated by the turbulent state of the boundary layer on the model base and flow rate coefficient increase with increased M_∞.

Conclusion

Tests of a three-dimensional inlet model demostrated the following results.

1) It was shown that the pitot and static pressure distributions were strongly nonuniform at the duct of the scramjet model.

2) It was established that such an inlet ensures a supersonic flow in the duct: in the flow core for $M_\infty \geq 3$ and on the wind-tunnel wall for $M_\infty \geq 4$ installed.

3) The significant effect of the thick boundary layer on the inlet starting, its integral performance, and dust flow was determined.

4) It was established that such an inlet has a sufficiently high level of pressure recovery coefficient at Mach number higher than 4.

5) It was established that such an inlet has a close to constant high level of flow rate at Mach number higher than 3.

At the same time, it was shown that additional efforts are needed to increase the total pressure recovery coefficient at $M_\infty < 4$ and the overall compression to ensure combustion.

Together with the data of Ref. 5 and 6, these results can be considered as a stage of studying a three-dimensional inlet for a scramjet. The testing of this model will be continued, extending the Mach number range and combustion experiments to study the ignition and combustion conditions for hydrogen and (or) hydrocarbon fuel.

References

[1]Goldfeld, M. A., "Experimental Study of 3D Inlets for High Supersonic Flight Velocities," *Proceedings of ICAR ITAM*, 1994, pp. 1–41.

[2]Gutov, B. I., and Zatoloka, V. V., "Convergent Inlet Diffusers with the Initial Shock and Additional External Compression," Inst. of Theoretical and Applied Mechanics, *Aerophisicheskie Issledovania*, Collection, No. 2, 1973, pp. 171–174 (in Russian).

[3]Gutov, B. I., and Zatoloka, V. V., "Design and Experimental Investigations of the Convergent Inlet Configuration with 3D Flow Combinations," Preprint 30–83, Inst. of Theoretical and Applied Mechanics, Siberian Branch, Novosibirsk, Russia, 1983 (in Russian).

[4]Trexler, C. A., "Inlet Performance of the Integrated Langley Scramjet Module (Mach 2.3 to 7.6)," AIAA Paper 75-1212, Oct. 1975.

[5]Vinogradov, V. A., Ogorodnikov, D. A., and Stepanov, V. A., "Experimental and Computational Researches of the Spatial (3-D) Hypersonic Inlets," AIAA Paper 98-1527, April 1998.

[6]Vinogradov, V. A., Goldfeld, M. A., and Stepanov, V. A., "Experimental and Numerical Investigation of Two Concepts of the Hypersonic Inlet," AIAA Paper 95-2721, July 1995.

[7]Goldfeld, M. A., "An Experimental Investigation of 3D Intakes for High Supersonic Flight Speeds," *Engine-Airframe Integration*, 1996, pp. 101–113.